Molecular Immunology 116 (2019) 29–37

Contents lists available at ScienceDirect

Molecular Immunology

journal homepage: www.elsevier.com/locate/molimm

Curcumin inhibits LPS-induced neuroinflammation by promoting microglial M2 polarization via TREM2/ TLR4/ NF-κB pathways in BV2 cells

Jiawei Zhang[1], Yaling Zheng[1], Yan Luo, Yu Du, Xiaojie Zhang, Jianliang Fu*

Department of Neurology, Shanghai Jiao Tong University Affiliated Sixth People's Hospital, 600 Yishan Road, Shanghai, 200233, China

ARTICLE INFO

Keywords:
Curcumin
Neuroinflammation
Microglia

ABSTRACT

Microglia mediate multiple facets of neuroinflammation, which plays a double-edged role in various brain diseases via distinct microglial phenotypes (deleterious M1 and neuroprotective M2). Therefore, the inhibition of overactivated inflammatory M1 microglia by switching to the protective M2 phenotype appears to be a potential therapeutic strategy in neuroinflammatory disorders. Curcumin has been shown to exhibit anti-inflammatory and neuroprotective activities. The present study investigated the potential effects of curcumin on microglial M1/M2 polarization and elucidated the possible molecular mechanisms of action in vitro. In this study, the BV2 microglial cell line was pretreated with different curcumin concentrations in the presence or absence of lipopolysaccharide (LPS) to assess the anti-inflammatory efficacy of curcumin based on the morphological and inflammatory changes. The cytotoxicity of curcumin for BV2 cells was evaluated using the CCK-8 assay. Further, the effect of curcumin concentrations on LPS-induced BV2 cells was studied. The morphological changes were observed using an optical microscope and immunofluorescent staining. Nitric oxide (NO) expression was determined using the Griess reagent. The expression of cytokines and inflammatory mediators was also measured by ELISA, qRT-PCR, flow cytometry, and immunofluorescence. Western blot analysis was used to determine the levels of triggering receptor expressed on myeloid cells 2 (TREM2), toll-like receptor 4 (TLR4), nuclear factor-kappa B (NF-κB) p65, p-NF-κB p65, IκB, and p-IκB expression. Results showed that curcumin concentrations less than 10 μM did not induce any detectable cytotoxicity but decreased BV2 cell viability up to 20 μM. Curcumin inhibited LPS-induced microglial activation. Curcumin treatment switched the M1 pro-inflammatory phenotype to the M2 anti-inflammatory phenotype by decreasing the expression of M1 markers (i.e., iNOS, IL-1β, IL-6, and CD16/32) and elevating the expression of M2 markers (i.e., arginase 1, IL-4, IL-10, and CD206). Interestingly, curcumin attenuated the activation of TLR4/NF-κB pathways and the downregulation of TREM2 expression in LPS-activated BV2 cells. Collectively, these results suggest that curcumin significantly alleviates LPS-induced inflammation by regulating microglial (M1/M2) polarization by reducing the imbalance of TREM2 and TLR4 and balancing the downstream NF-κB activation.

1. Introduction

Emerging evidence suggests that neuroinflammation is a significant and inevitable pathological process mediating all types of damage and disorders of central nervous system (CNS) (Yang and Zhou, 2019). Microglia, the major cellular elements of neuroinflammation, serve as tissue-resident macrophages influencing brain development, maintenance of neural environment, and response to injury and repair. Under normal physiological conditions, microglia assume a relatively quiescent surveillance phenotype to monitor the microenvironment of parenchyma continuously. However, when the immune homeostasis is disturbed, microglia can be phenotypically transformed into two extremes of polarization: the classically activated M1 (pro-inflammatory) and alternatively activated M2 (anti-inflammatory) phenotypes. The different microglial phenotypes play an important role in regulating the occurrence, development, and cessation of inflammatory diseases. Activated M1 microglia are characterized by the increased release of pro-inflammatory factors, including tumor necrosis factor-α (TNF-α), interleukin-1β (IL-1β), interleukin-6 (IL-6), and the up-regulation of inducible nitric oxide synthase (iNOS), CD16/32, and CD68, which elicit detrimental effects on neurons and further exacerbate tissue inflammation and damage. By contrast, the activated M2 microglia upregulate the expression of anti-inflammatory mediators and neurotrophic factors, such as transforming growth factor-β, interleukin-

* Corresponding author.
E-mail address: fujianliang@163.com (J. Fu).
[1] Jiawei Zhang and Yaling Zheng contributed equally to this work.

https://doi.org/10.1016/j.molimm.2019.09.020
Received 22 May 2019; Received in revised form 16 August 2019; Accepted 26 September 2019
Available online 04 October 2019

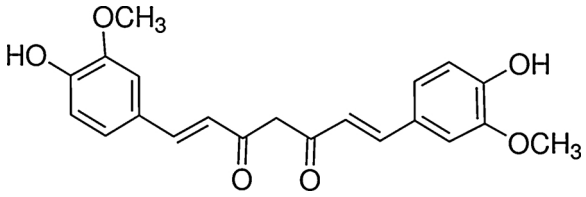

Fig. 1. Chemical structure of curcumin.

10 (IL-10), arginase-1 (Arg-1), and CD206, which lead to neuroprotection and facilitate recovery and remodeling (Dong et al., 2019; Subhramanyam et al., 2019). Therefore, inhibition of the M1 phenotype while stimulating the M2 phenotype has been suggested as a potential therapeutic approach compared with inhibition of M1 activation alone for the treatment of neuroinflammatory diseases. Recently, several plant-derived compounds have been shown to combat neuroinflammation and tissue damage in cerebral diseases (Jin et al., 2019b; Li et al., 2018). However, drug-induced polarization of the microglia from the M1 phenotype to the M2 phenotype is rare.

Curcumin (1,7-bis[4-hydroxy-3-methoxyphenyl]-1,6-heptadiene-3,5-dione, Fig. 1), the main bioactive component occurring in the rhizome of turmeric (Curcuma longa), is widely recognized for its anti-inflammatory, antioxidant, and anti-tumor activities (Hussain et al., 2017; Kreutz et al., 2018; Li et al., 2017). Many studies have reported the neuroprotective effect of curcumin in animal models of neurodegenerative diseases, such as Alzheimer's disease (AD), Parkinson's disease (PD), multiple sclerosis, and depression (Ghanaatian et al., 2019; Tang and Taghibiglou, 2017; Tizabi et al., 2014). Our previous study has also demonstrated the protective role of curcumin against ischemic stroke in experimental models (Zhang et al., 2018b). However, whether curcumin inhibits the polarization of LPS-induced microglial phenotype and promotes microglial polarization to M2 phenotype remains unclear. Moreover, the molecular mechanisms underlying curcumin-mediated anti-neuroinflammatory eff ;ects remain unknown.

A number of signaling molecules, including TLR4/NF-κB and TREM2, are critical to the modulation of microglial activation and neuroinflammation. TLR4 is predominantly expressed in the microglia of the brain and stimulated by appropriate ligands, including lipopolysaccharide (LPS). Stimulation of TLR4 further activates the NF-κB pathway, which plays an important role in the activation of M1 microglia and induces the transcription of pro-inflammatory cytokines, including interleukin-1β (IL-1β), interleukin-6 (IL-6), and tumor necrosis factor-α (TNF-α) (Shi et al., 2019; Wan et al., 2016). TREM2 is an important innate immune receptor uniquely expressed on the microglia and is involved in down-regulating neuroinflammation in the CNS (Andreasson et al., 2016). We investigated whether the imbalance between microglial TLR4 and TREM2 mediated microglial polarization and neuroinflammation in LPS-induced BV2 cells. In the current study, we analyzed the potential eff ;ects of curcumin on microglial M1/M2 polarization and further elucidated the underlying mechanisms of action.

2. Materials and methods

2.1. Materials

BV2 mouse microglial line, fetal bovine serum (FBS), and 1% penicillin–streptomycin were purchased from ScienCell (CA, USA). Curcumin and LPS were obtained from Sigma. Enzyme-linked immunosorbent assay (ELISA) kits for IL-1β and IL-10 were purchased from Anogen. NO assay kit and RNAeasy™ animal RNA isolation kit with spin column were from Beyotime. TB Green™ Premix Ex Taq™ II (Tli RNaseH Plus) and PrimeScript™ RT Master Mix (Perfect Real Time) were purchased from Takara (Japan). Cell Counting Kit-8 assay (CCK-8) was acquired from Dojindo. Antibodies against beta-actin, HRP-conjugated AffiniPure Goat Anti-Mouse IgG (H + L) and HRP-conjugated Affinipure Goat Anti-Rabbit IgG(H + L) were obtained from Proteintech. Antibodies targeting Iba-1, TREM2, iNOS CD206 and donkey anti-goat AlexFluor 555®, donkey anti- rabbit AlexFluor 488®, and donkey anti-rabbit Alex Fluor 555® secondary antibodies were obtained from Abcam. Antibodies for IκB-α, p-IκB-α, NF-κB p65, and p-NF-κB p65 were supplied by Cell Signaling. Antibodies for TLR4 were acquired from Santa Cruz Biotechnology. Anti-mo CD206 MR6F3 PE and Ms CD16/CD32 APC were purchased from eBiosciences.

2.2. Cell culture and treatment

Immortalized mouse BV2 microglial cell lines were cultured in MEM medium with 10% FBS and 1% penicillin/streptomycin at 37 °C in a humidified atmosphere containing 95% air and 5% CO2, and the medium was changed every two days. The cells were split with 0.25% trypsin when they reached 80% confluence and sub-cultured for further passages. Cells were pretreated with various concentrations of curcumin (1,5, 10, 20, and 40 μM) for 2 h, and treated with or without LPS (1 μg/mL) for 24 h.

2.3. Cell viability assay and morphological analysis

Cell viability was assessed with the CCK-8 assay using a 96-well culture plate, as described previously (Shi et al., 2019). Briefly, BV2 cells were seeded and treated with diff ;erent concentrations of curcumin in the presence or absence of LPS for 24 h. CCK-8 solution (10 μL) was added to each well. After incubation for 2 h at 37 °C, the absorbance at 450 nm was read on a microplate reader (Thermo Scientific). For morphological analysis, cells were imaged with the Olympus microscope system (Olympus, Tokyo, Japan) at 20× magnification.

2.4. NO assay

Microglial production of NO was assessed by measuring the accumulated nitrite released into culture media. A cell suspension was prepared by seeding BV2 microglial cells in the logarithmic growth phase into a 6-well culture plate at a density of 1×10^6 cells/well (2 mL medium/well). After 24 h, cells were pretreated with different concentrations of curcumin (1, 5, and 10 μM) for 2 h, and incubated with or without LPS (1 μg/mL) for 24 h. The supernatant was collected, and NO production was determined using a NO assay kit protocol. The absorbance of the reaction mixtures was measured at 540 nm using a microplate reader (Thermo Scientific).

2.5. Flow cytometry

Cells were plated in 6-well dishes at a density of 1×10^6 per well and incubated as aforementioned for 24 h. After the addition of curcumin for 2 h, LPS was added to each well and the cells were incubated for an additional 24 h. The cells in the culture dish were digested using trypsin, and washed and re-suspended in cold PBS at a density of (1–3) $\times$ 10^6 cells/mL. The membrane proteins CD16/32 and CD206 were detected by direct immunofluorescence staining. The cells were incubated with APC-conjugated monoclonal mouse CD16/32 antibodies or PE-conjugated monoclonal mouse CD206 antibodies at room temperature in the dark for 30 min. The cells were washed twice with PBS and re-suspended in 500 μL of 1 × PBS solution. APC and PE-conjugated monoclonal antibodies with irrelevant specificity were used as negative controls. Light scatter characteristics of each sample (10^5 cells) were analyzed using flow cytometry (CytoFLEX LX, USA).

2.6. ELISA for the determination of cytokine levels

A cell suspension was prepared by inoculating BV2 microglial cells

Table 1
Primers for qPCR.

Gene	Sense (5′-3)	Anti-sense (5′-3)
IL-1β	TTTGAAGTTGACGGACCCCAA	CACAGCTTCTCCACAGCCACA
IL-4	ATCGGCATTTTGAACGAGGTCACA	CGAAGCACCTTGGAAGCCCTA
IL-6	TTCTTGGGACTGATGCTGGTG	CACAACTCTTTTCTCATTTCCACGA
IL-10	TTACCTGGTAGAAGTGATGCCC	GACACCTTGGTCTTGGAGCTTA
Arg-1	AGGAAAGCTGGTCTGCTGGAA	AGATGCTTCCAACTGCCAGAC
iNOS	GGGCTGTCACGGAGATCAATG	GCCCGGTACTCATTCTGCATG
Actin	CTGAGAGGGAAATCGTGCGT	CCACAGGATTCCATACCCAAGA

in the logarithmic growth phase into a 6-well culture plate. After 24 h, cells were pretreated with different concentrations of curcumin (1, 5, and 10 μM) for 2 h, and incubated with or without LPS (1 μg/mL) for 24 h. The supernatant was collected, and the concentrations of IL-1β and IL-10 levels were measured by ELISA according to the manufacturer's instructions. Optical density (OD) was measured at 450 nm using a microplate reader (Thermo Scientific).

2.7. Quantitative PCR (qPCR) assay

Total RNA was extracted using the RNAeasy™ animal RNA isolation kit with a spin column according to the manufacturer's protocol. Isolated RNA was reverse-transcribed into cDNA using the PrimeScript™ RT Master Mix (Perfect Real Time) following the standard protocol. The qPCR assay was conducted using TB Green™ Premix Ex Taq™ II (Tli RNaseH Plus) with the Applied Biosystems 7500 Real-Time PCR System (Applied Biosystems, United States). The amplification parameters were 95 °C for 30 s, followed by 40 cycles of 95 °C for 5 s and 60 °C for 34 s, 95 °C for 15 s, 60 °C for 60 s, and 95 °C for 15 s. Each sample was analyzed in triplicate, and the relative expression of mRNA was calculated after normalization to β-actin. All primer sequences used are listed in Table 1.

2.8. Western blot analysis

Cells were seeded in T25 flasks, and incubated and treated as mentioned above. Cultured cells were lysed with RIPA buff ;er supplemented with protease and phosphatase inhibitors, scraped off ; the flasks, and collected for protein extraction. The lysates were incubated on ice for 10 min and centrifuged at 12,000 rpm for 5 min at 4 °C, and the supernatants were collected. The protein concentration was determined using a BCA kit. Proteins (30 μg) were separated by sodium dodecyl sulphate-polyacrylamide gel electrophoresis (SDS-PAGE) and transferred to polyvinylidene fluoride (PVDF) membranes for 60 min at 250 mA. After blocking with 5% non-fat milk or BSA for 2 h in TBS-T, the membrane was incubated overnight with primary antibodies (TREM2, 1:500; TLR4, 1:500; IκBα, 1:1000; p-IκBα, 1:1000; NF-κB, 1:1000; p-NF-κB, 1:1000; β-actin, 1:1000) in TBS-T at 4 °C overnight. On the next day, the membrane was washed three times for 10 min each with TBS-T buff ;er, and incubated for 60 min with anti-rabbit or anti-mouse horseradish peroxidase (HRP)-conjugated immunoglobulin G (IgG) secondary antibodies diluted in TBS-T (1:3000). Finally, the membrane was washed three times for 10 min each, with TBS-T buff ;er. The protein bands were detected with enhanced chemiluminescence (ECL). Digital images were analyzed using Quantity One to obtain the grey-scale value of signals. β-actin was used as an internal reference.

2.9. Immunofluorescence staining

A slide coated with poly L-lysine (0.1 mg/mL) was placed in a 24-well plate. BV2 cells were cultured and treated as indicated, and fixed with 4% paraformaldehyde for 30 min at room temperature followed by permeabilization using 0.3% Triton X-100 for 15 min. The cells were blocked with PBS containing 3% donkey serum for 1 h. The cells were incubated with anti-goat Iba-1 (1:200), anti-rabbit TREM2 (1:200), anti-rabbit CD206 (1:500), and anti-rabbit iNOS (1:100) at 4 °C overnight. On the following day, cells were washed with PBS and incubated with donkey anti-goat AlexFluor 555® (1:500), donkey anti- rabbit AlexFluor 488® (1:500), and donkey anti-rabbit Alex Fluor 555® (1:500) secondary antibodies for 1 h. The cells were treated with an anti-fade mounting medium with DAPI for 10 min at 37 °C. All images were captured with a fluorescence microscope (Olympus, Japan).

2.10. Phagocytosis assay

The microglial phagocytosis was evaluated by imaging analysis with latex beads. Briefly, BV-2 cells were re-plated on glass coverslips in 12-well tissue culture dishes (5×10^4 cells/dish). Pre-opsonize aqueous green fluorescent latex beads in FBS for 1 h at 37 °C. The ratio of beads to FBS is 1:5. Dilute the bead-containing FBS with DMEM to reach the final concentrations for beads and FBS in DMEM of 0.01% (v/v) and 0.05% (v/v), respectively. Replace microglial conditioned culture media with beads-containing DMEM and incubate cultures at 37 °C for 1 h. Then, the BV-2 cells were thoroughly washed with PBS to remove any extracellular beads before being fixed in 4% paraformaldehyde. After washing again with PBS, the BV-2 cells were blocked for 1 h with blocking solution (1% BSA, 0.3% Triton in PBS). The cells were incubated with anti-Iba1 antibody (1:500) for 1 h. After the 1-h incubation, the cells were washed with PBS and incubated with donkey anti-goat AlexFluor 555® (1:500) for 1 h. Finally, the coverslips were mounted with DAPI. BV-2 cells were examined under a microscope to determine whether the fluorescent beads had been phagocytosed and were present inside the cells.

2.11. Statistical analysis

Data are reported as mean ± standard error of the mean (SEM) from three independent experiments, each performed in triplicate. Data analysis was performed using one-way analysis of variance (ANOVA) with SPSS 23.0, followed by Tukey post-hoc test. $P < 0.05$ was considered statistically significant.

3. Results

3.1. Effects of curcumin on the viability of BV2 cells and microglial activation

To determine whether curcumin influences the viability of BV2 cells, the cell counting kit-8 (CCK-8) assay was performed 24 h after treatment with various concentrations of curcumin ranging from 1 μM to 40 μM. Results (Fig. 2A) showed that curcumin concentrations less than 10 μM alone did not induce any detectable cytotoxicity but decreased BV2 cell viability and induced cytotoxicity at 20 μM concentration. Thus, the concentrations of curcumin ranging from 1 to 10 μM were used in subsequent experiments. The BV2 cells were pretreated with different concentrations of curcumin for 2 h, and incubated for 24 h with or without LPS (1 μg/mL). Curcumin at different concentrations (1, 5, and 10 μM) showed no significant toxic eff ;ects on

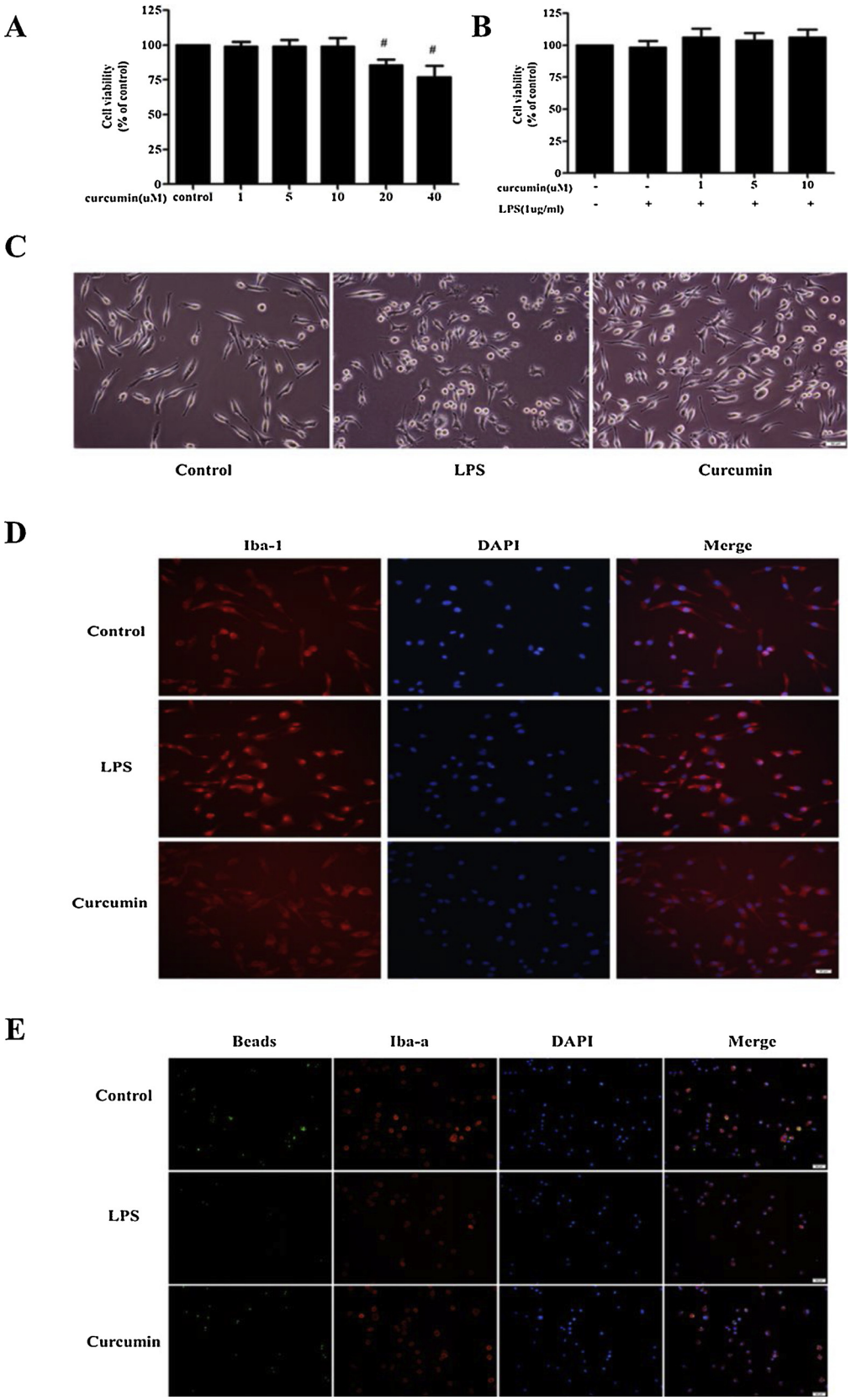

Fig. 2. Effects of curcumin on the viability and activation of BV2 cells with or without LPS stimulation. Effects of different concentrations of curcumin alone on cell viability (A). BV2 cells were pretreated with different concentrations of curcumin for 2 h and incubated with or without LPS (1 μg/mL) for 24 h. Cell viability was determined using CCK-8 assay (B); cell morphology was observed with an optical microscope (C), and immunostaining (D). Representative photomicrographs showed BV-2 cells containing phagocytosed fluorescent beads (green) immunolabeled using an anti-ionized calcium-binding adaptor protein 1 (Iba1) antibody (red). Nuclei were stained with DAPI (blue). Data are presented as the means ± SEM from three independent experiments performed in triplicate. $^{\#}p < 0.05$ compared with the control group. $^{*}p < 0.05$ compared with the LPS-treated group. Scale bar = 50 μm. (For interpretation of the references to colour in this figure legend, the reader is referred to the web version of this article).

cell viability (Fig. 2B).

To investigate the eff ;ects of curcumin on LPS-induced microglial activation, the morphological changes and phagocytic activity in BV2 cells were evaluated after treatment with curcumin (5 μM) with or without LPS. As indicated in Fig. 2C and 2D, both microscopic and immunostaining results using an anti-Iba-1 (a specific microglial marker) antibody showed that the resting microglia were spindle-shaped with small cell bodies and long processes. After treatment with

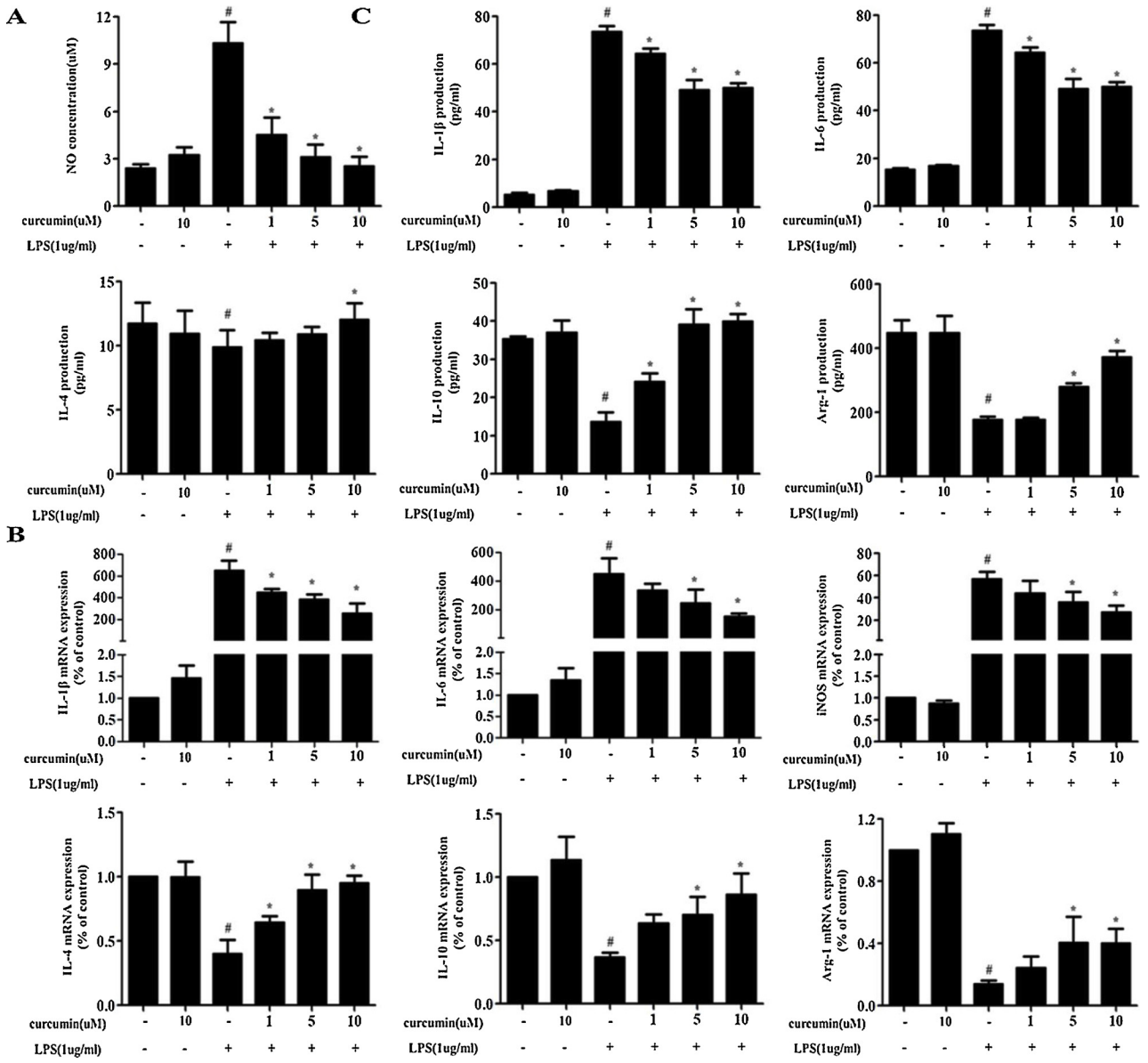

Fig. 3. Eff ;ects of curcumin on LPS-induced NO production and inflammatory cytokine production. BV2 cells were pretreated with various concentrations of curcumin for 2 h and incubated with or without LPS (1 μg/mL) for 24 h. (A) NO concentration in the supernatant was measured using the Griess reaction. Levels of IL-1β, IL-6, IL-4, IL-10, and Arg-1 in the supernatants were determined by ELISA, and the whole cells were collected to determine the gene expression of IL-1β, IL-6, iNOS, IL-4, IL-10, and Arg-1 using real time RT-PCR (B,C). Data are presented as the means ± SEM of three independent experiments. $^{\#}p < 0.05$ compared with the control group. $^{*}p < 0.05$ compared with the LPS-treated group.

LPS, the microglia acquired a pro-inflammatory M1 amoeboid morphology, characterized by thick and short cell bodies. However, LPS-induced morphological changes in BV2 cells were attenuated after treatment with curcumin. Surprisingly, the number of cells containing phagocytosed beads decreased after LPS stimulation in comparison to control, but this number was reduced by curcumin (Fig. 2E). These results suggest that optimal concentration of curcumin could reverse LPS-induced phagocytic activity decreased and morphological changes.

3.2. Effects of curcumin on the production of NO and inflammatory cytokines in LPS-induced BV2 cells

BV2 cells were pretreated with different concentrations of curcumin for 2 h, and incubated for 24 h with or without LPS. To determine the effects of curcumin on LPS-induced inflammatory mediators, we initially evaluated the production of NO. Results showed (Fig. 3A) that NO level was significantly increased after LPS treatment, compared with the control group. Interestingly, curcumin (1–10 μM) reduced NO levels in a dose-dependent manner. Both ELISA and qRT-PCR were used to investigate whether curcumin regulated the expression of inflammatory cytokines. The LPS-induced production of IL-1β, IL-4, iNOS, IL-6, IL-10, and Arg-1 was measured by qRT-PCR. Results showed (Fig. 3B) that the level of M1 pro-inflammatory cytokines was greatly increased by LPS stimulation, as evidenced by the production of IL-1β, IL-6, and iNOS. The M2 anti-inflammatory cytokines (IL-6, IL-10, and Arg-1) were decreased after LPS stimulation. Importantly, curcumin treatment inhibited LPS-induced M1 pro-inflammatory cytokine (IL-1β, IL-6, and iNOS) synthesis whereas the production of M2 anti-inflammatory cytokines (IL-6, IL-10, and Arg-1) was increased in a dose-dependent manner. Consistent with the results of qRT-PCR analysis, ELISA showed that treatment with LPS significantly increased the level of pro-inflammatory cytokines (IL-1β and IL-6) while the anti-inflammatory cytokine (IL-10, IL-4, and Arg-1) level was markedly decreased. Interestingly, the expression of pro-inflammatory and anti-

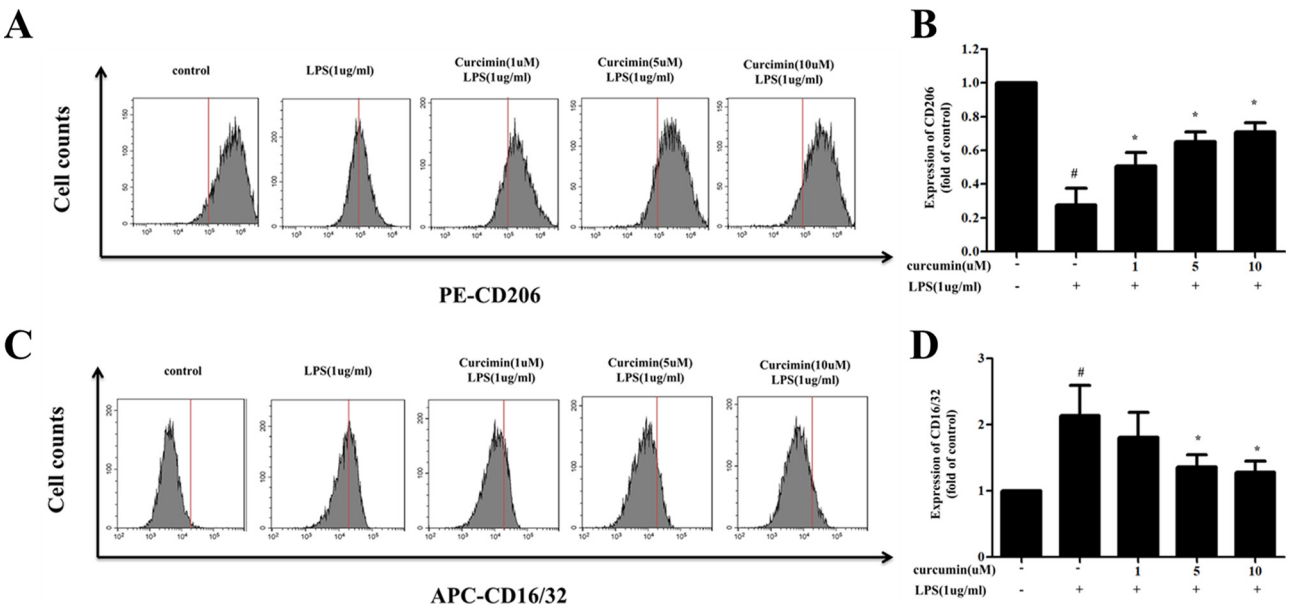

Fig. 4. Eff ;ects of curcumin on LPS-induced protein expression of CD206 and CD16/32 in BV2 cells. The cells were pretreated with different concentrations of curcumin 2 h, and incubated with or without LPS (1 μg/mL) for 24 h. (A, B) CD206 (M2) and (C, D) CD16/32 (M1) protein expression was measured via flow cytometry. Data are presented as the means ± SEM of three independent experiments. $^{\#}p < 0.05$ compared with the control group. $^{*}p < 0.05$ compared with the LPS-treated group.

inflammatory cytokines was significantly and dose-dependently reversed in the presence of curcumin (Fig. 3C). These results indicate that curcumin exhibited anti-inflammatory effects in LPS-stimulated BV2 cells.

3.3. Curcumin promoted microglial polarization to the M2 phenotype in LPS-induced BV2 cells

CD16/32 and iNOS were used as the markers of M1 polarization, while CD206 was employed as the marker of M2 polarization. To evaluate whether the neuroprotective eff ;ect of curcumin was associated with BV2 cell polarization, we measured the expression of CD16/32 and CD206 via flow cytometry to determine the effect of curcumin on phenotype switch in BV2 cells. As shown in Fig. 4A–D, the protein expression of CD16/32 was markedly downregulated by curcumin pretreatment, compared with that of the LPS group. Curcumin pretreatment greatly increased the expression of CD206 in BV2 cells compared with the LPS group. To further determine whether curcumin switched microglial phenotype from M1 to M2, we measured the expression of iNOS and CD206. As shown in Fig. 5A–D, higher levels of iNOS immunoreactivity and diminished CD206 immunoreactivity were detected in LPS-treated cultures, compared with the control group. Curcumin pretreatment decreased iNOS immunoreactivity and increased CD206 immunoreactivity.

3.4. Effects of curcumin on LPS-induced TREM2/TLR4/NF-κB pathways

It has been reported both TLR4 and TREM2 are microglial membrane receptors that play an important role in signaling pathways mediating inflammation. Because LPS may induce neuroinflammation via interaction with microglial membrane receptors, we first determined the levels of two key regulators, TLR4 and TREM2, in LPS-treated BV2 cells. As shown in Fig. 6A, the western blot showed a persistent upregulation of TLR4 expression, and interestingly, a significant downregulation of TREM2 expression in LPS-treated BV2 cells compared with the control group. However, curcumin pretreatment effectively inhibited TLR4 expression, but increased TREM2 expression. Because the activation of NF-κB by LPS induced the expression of pro-inflammatory cytokines, we evaluated the effects of curcumin on NF-κB pathway via western blotting analysis. As shown in Fig. 6B and C, LPS stimulation resulted in the phosphorylation of IκB-α, and NF-κB p65 without affecting the expression of IκB-α and NF-κB p-65. However, curcumin pretreatment decreased the expression of p-IκB-α and p-NF-κB p65. Together, these results indicate that curcumin abrogated the LPS-induced imbalance of TREM2 and TLR4 by balancing the downstream NF-κB activation, which may probably contribute to the over-activation of microglia.

4. Discussion

Recently, several phytochemicals have been comprehensively investigated for their potential neuroprotective effects in various neurological disorders (Costa et al., 2018; Patel and Udayabanu, 2017). Curcumin, isolated from *Curcuma longa,* is a highly pleiotropic molecule with numerous biological properties including anti-inflammatory, anti-oxidative, and anti-cancer activities. Extensive preclinical trials have indicated the therapeutic potential of curcumin against a wide range of human diseases (Abrahams et al., 2019; Bielak-Zmijewska et al., 2019; Ghasemi et al., 2019). In this study, we explored the anti-inflammatory properties of curcumin against LPS-induced neuroinflammation by regulating microglial M1/M2 polarization by reducing the imbalance of TREM2-TLR4-mediated NF-κB signaling pathway.

Increasing evidence has confirmed the ubiquitous role of neuroinflammation in the pathogenesis of neurological disorders, including Alzheimer's disease (AD), Parkinson's disease (PD), ischemic stroke, experimental autoimmune encephalomyelitis (EAE), and amyotrophic lateral sclerosis (Jin et al., 2019a; Ravelli et al., 2019; Sharman et al., 2019). Neuroinflammation is a double-edged sword in CNS diseases. Acute neuroinflammation plays a protective role by scavenging harmful substances in the body via microglial phagocytosis while chronic neuroinflammation is always detrimental to nervous tissue due to the release of various pro-inflammatory and cytotoxic factors (Block, 2014). Thus, whether neuroinflammation has beneficial or harmful effects on CNS may critically depend on the duration of the inflammatory response and the type of microglia activation.

Microglia are highly plastic cells, and classification of activated microglia into the classical pro-inflammatory M1 phenotype and the alternative immunosuppressive M2 phenotype is an oversimplification.

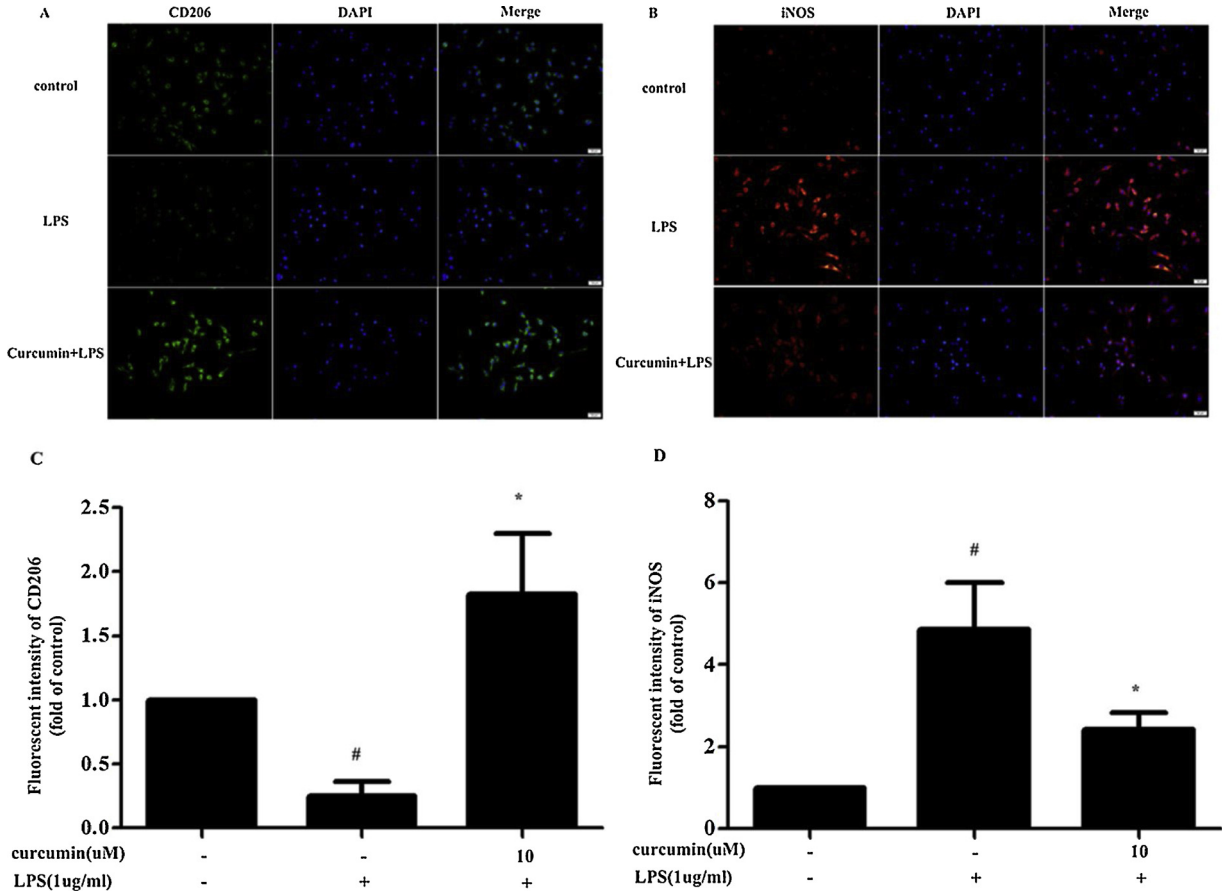

Fig. 5. Curcumin switched microglial polarization from M1 to M2 in LPS-induced BV2 cells. Cells were pretreated with curcumin for 2 h, and incubated with or without LPS (1 μg/mL) for 24 h. Cultures were visualized via immunostaining with anti-iNOS (M1 marker, red) and anti-CD206 (M2 marker, green) antibodies (A,B). Nuclei were stained with DAPI (blue). (C,D) Representative images of fluorescence intensity of CD206 and iNOS with or without LPS treatment. Data are presented as the means ± SEM of three independent experiments. $^{\#}p < 0.05$ compared with the control group. $^{*}p < 0.05$ compared with the LPS-treated group. Scale bar = 50 μm. (For interpretation of the references to colour in this figure legend, the reader is referred to the web version of this article).

The M1/M2 paradigm merely represents a simplified model of two polar extremes of inflammatory response (Gaikwad and Heneka, 2013; Ransohoff, 2016; Tang and Le, 2016). However, it is the most commonly used approach to elucidate the role of microglia in several brain diseases. Typically, the activated M1 phenotype can be induced in vitro by LPS to express various pro-inflammatory factors such as IL- 1β, iNOS, and CD16. In contrast, IL-4 has been shown to induce the activated M2 phenotype, which is characterized by the expression of anti-inflammatory and neurotrophic mediators such as IL-10, arg-1, and CD206 (Cianciulli et al., 2016; Wu et al., 2018; Zhang et al., 2018a). Based on previous anti-inflammatory prevention trials using non-steroidal anti-inflammatory drugs (NSAIDs) and AD, the shift towards pro-inflammatory M1 phenotype is not likely to result in overall benefits (Cote et al., 2012; Lehrer and Rheinstein, 2015). Following stimulation, microglia dynamically switch between M1 and M2 phenotypes resulting in neurotoxic and neuroprotective effects, respectively. Accordingly, a timely shift of microglial M1 to M2 phenotype has been regarded as a promising strategy for the management of neuroinflammation-related disorders. Recent studies have increasingly found that the regulation of microglial M1/M2 polarization creates a microenvironment conducive to CNS recovery by suppressing the deleterious effects of inflammation, while boosting the neuroprotective potential. For instance, IL-4 treatment was shown to enhance M2 microglial polarization and improve the outcomes of focal cerebral ischemia (Xiong et al., 2015; Yang et al., 2016). Additional studies have shown that enhanced M2 microglia polarization correlated with better clearance of Aβ plaques in AD and decreased neurodegeneration in PD (Yan et al., 2018; Zhang and He, 2017).

Thus, our study focused on the role of curcumin in the modulation of microglial polarization. In the present in vitro study, we found that LPS-induced M1 polarization led to a marked increase in NO release, IL-1β, IL-6, CD16/32, iNOS mRNA, and protein expression and intense iNOS staining, while treatment with curcumin prior to LPS stimulation reversed the M1 polarization and strongly increased the expression of the M2 microglial markers, IL-4, IL-10, CD206, and arg-1. Collectively, these results indicated that curcumin switched the polarization of LPS-activated BV2 microglia from M1 to a predominantly M2 phenotype, which was correlated with a significant decrease in neurotoxicity and enhanced anti-inflammatory cytokine production. However, the molecular mechanism by which curcumin induces changes in microglial polarization remains unclear.

LPS is a component of the outer membrane of Gram-negative bacteria that acts as a TLR4 ligand to further induce various downstream signal pathways such as NF-κB (Nair et al., 2019). As a key transcription factor, NF-κB plays an important role in the expression of pro-inflammatory cytokines. Usually, inactivated NF-κB is located in the cytoplasm bound to the inhibitor of IκB. Activation by inflammatory stimuli, such as LPS, strongly enhances the phosphorylation and proteasomal degradation of the IκB inhibitory proteins, resulting in the release and nuclear translocation of NF-κB (Kim et al., 2019). Recently, several studies indicated that TREM2 is an efficient negative regulator of TLR4 signaling (Gawish et al., 2015; Rosciszewski et al., 2018; Zhou et al., 2019). As a membrane receptor primarily expressed in microglial cells within the CNS, TREM2 mediates critical functions of microglia,

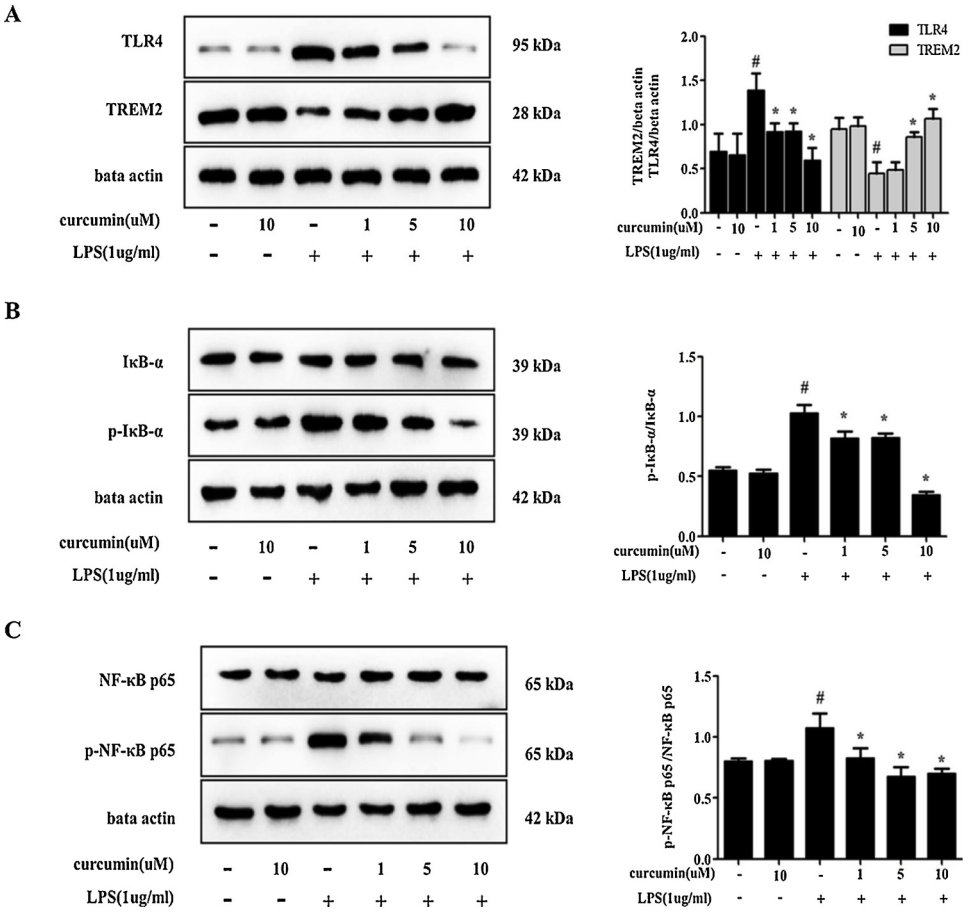

Fig. 6. Effects of curcumin on LPS-induced TREM2/TLR4/NF-κB signal transduction in BV2 cells. Cells were pretreated with different concentrations of curcumin for 2 h, and incubated with or without LPS (1 μg/mL) for 24 h. Cultures were harvested to determine the protein expression of TREM2, TLR4, IκB-α, P-IκB-α, NF-κB p-65, and p-NF-κB p-65 via western blot analysis. (A) Determination of TREM2 and TLR4 protein levels by western blot. (B,C) Determination of IκB-α, P-IκB-α, NF-κB p-65, and p-NF-κB p-65 protein levels by western blot analysis. Data are presented as the means ± SEM of three independent experiments. $^{\#}p < 0.05$ compared with the control group. $^{*}p < 0.05$ compared with the LPS-treated group.

such as suppression of pro-inflammatory cytokines and promotion of phagocytosis of apoptotic neurons and cell debris (Takahashi et al., 2005). In macrophages or dendritic cells, the reduced TREM2 expression enhanced inflammatory cytokine production after TLR activation (Hamerman et al., 2006; Ito and Hamerman, 2012). Moreover, in vivo studies suggested that TREM2 modulated neuroinflammatory responses by negatively regulating the TLR4-mediated activation of NF-κB signaling pathways (Ren et al., 2018). Therefore, we investigated whether the activation of TREM2 via TLR4/NF-κB suppression confers neuroprotective effects against LPS-induced neuroinflammatory responses in BV2 cells. As expected, the results demonstrated that LPS effectively enhanced the expression of TLR4, the degradation and phosphorylation of IκBα, and the phosphorylation of NF-κB p65 in BV2 cells, but significantly decreased TREM2 expression. However, curcumin administration effectively reversed LPS-induced hyperactivity of TLR4 and NF-κB by markedly increasing TREM2 expression in BV2 cells. Thus, curcumin inhibits LPS-induced neuroinflammatory response by reducing the imbalance of TREM2 and TLR4-mediated NF-κB activation.

In summary, the present study demonstrates for the first time that curcumin facilitates microglial polarization from the pro-inflammatory phenotype towards the anti-inflammatory phenotype by overcoming the imbalance between TREM2 and TLR4 via balanced downstream NF-κB activation. This study provides novel insights into the role of curcumin treatment in microglia-mediated neuroinflammatory diseases.

Declaration of Competing Interest

The authors declare that they have no conflict of interest.

Acknowledgement

This study was supported by the Project of National Natural Science Foundation of China (No.81871103, No.81672243).

References

Abrahams, S., Haylett, W.L., Johnson, G., Carr, J.A., Bardien, S., 2019. Antioxidant effects of curcumin in models of neurodegeneration, aging, oxidative and nitrosative stress: a review. Neuroscience 406, 1–21.
Andreasson, K.I., Bachstetter, A.D., Colonna, M., Ginhoux, F., Holmes, C., Lamb, B., Landreth, G., Lee, D.C., Low, D., Lynch, M.A., Monsonego, A., O'Banion, M.K., Pekny, M., Puschmann, T., Russek-Blum, N., Sandusky, L.A., Selenica, M.L., Takata, K., Teeling, J., Town, T., Van Eldik, L.J., 2016. Targeting innate immunity for neurodegenerative disorders of the central nervous system. J. Neurochem. 138, 653–693.
Bielak-Zmijewska, A., Grabowska, W., Ciolko, A., Bojko, A., Mosieniak, G., Bijoch, L., Sikora, E., 2019. The role of curcumin in the modulation of ageing. Int. J. Mol. Sci. 20.
Block, M.L., 2014. Neuroinflammation: modulating mighty microglia. Nat. Chem. Biol. 10, 988–989.
Cianciulli, A., Calvello, R., Porro, C., Trotta, T., Salvatore, R., Panaro, M.A., 2016. PI3k/Akt signalling pathway plays a crucial role in the anti-inflammatory effects of curcumin in LPS-activated microglia. Int. Immunopharmacol. 36, 282–290.
Costa, I.M., Lima, F.O.V., Fernandes, L.C.B., Norrara, B., Neta, F.I., Alves, R.D., Cavalcanti, J., Lucena, E.E.S., Cavalcante, J.S., Rego, A.C.M., Filho, I.A., Queiroz, D.B., Freire, M.A.M., Guzen, F.P., 2018. Astragaloside IV supplementation promotes a neuroprotective effect in experimental models of neurological disorders: a systematic review. Curr. Neuropharmacol.
Cote, S., Carmichael, P.H., Verreault, R., Lindsay, J., Lefebvre, J., Laurin, D., 2012. Nonsteroidal anti-inflammatory drug use and the risk of cognitive impairment and Alzheimer's disease. Alzheimers Dement. 8, 219–226.
Dong, Y., Li, X., Cheng, J., Hou, L., 2019. Drug Development for Alzheimer's Disease: Microglia Induced Neuroinflammation as a Target? Int. J. Mol. Sci. 20.
Gaikwad, S.M., Heneka, M.T., 2013. Studying M1 and M2 states in adult microglia. Methods Mol. Biol. 1041, 185–197.
Gawish, R., Martins, R., Bohm, B., Wimberger, T., Sharif, O., Lakovits, K., Schmidt, M., Knapp, S., 2015. Triggering receptor expressed on myeloid cells-2 fine-tunes inflammatory responses in murine Gram-negative sepsis. FASEB J. 29, 1247–1257.
Ghanaatian, N., Lashgari, N.A., Abdolghaffari, A.H., Rajaee, S.M., Panahi, Y., Barreto,

G.E., Butler, A.E., Sahebkar, A., 2019. Curcumin as a therapeutic candidate for multiple sclerosis: molecular mechanisms and targets. J. Cell. Physiol. 234, 12237–12248.
Ghasemi, F., Bagheri, H., Barreto, G.E., Read, M.I., Sahebkar, A., 2019. Effects of curcumin on microglial cells. Neurotox. Res.
Hamerman, J.A., Jarjoura, J.R., Humphrey, M.B., Nakamura, M.C., Seaman, W.E., Lanier, L.L., 2006. Cutting edge: inhibition of TLR and FcR responses in macrophages by triggering receptor expressed on myeloid cells (TREM)-2 and DAP12. J. Immunol. 177, 2051–2055.
Hussain, Z., Thu, H.E., Amjad, M.W., Hussain, F., Ahmed, T.A., Khan, S., 2017. Exploring recent developments to improve antioxidant, anti-inflammatory and antimicrobial efficacy of curcumin: a review of new trends and future perspectives. Mater. Sci. Eng. C Mater. Biol. Appl. 77, 1316–1326.
Ito, H., Hamerman, J.A., 2012. TREM-2, triggering receptor expressed on myeloid cell-2, negatively regulates TLR responses in dendritic cells. Eur. J. Immunol. 42, 176–185.
Jin, X., Liu, M.Y., Zhang, D.F., Zhong, X., Du, K., Qian, P., Gao, H., Wei, M.J., 2019a. Natural products as a potential modulator of microglial polarization in neurodegenerative diseases. Pharmacol. Res. 145, 104253.
Jin, X., Liu, M.Y., Zhang, D.F., Zhong, X., Du, K., Qian, P., Yao, W.F., Gao, H., Wei, M.J., 2019b. Baicalin mitigates cognitive impairment and protects neurons from microglia-mediated neuroinflammation via suppressing NLRP3 inflammasomes and TLR4/NF-kappaB signaling pathway. CNS Neurosci. Ther. 25, 575–590.
Kim, M.E., Park, P.R., Na, J.Y., Jung, I., Cho, J.H., Lee, J.S., 2019. Anti-neuroinflammatory effects of galangin in LPS-stimulated BV-2 microglia through regulation of IL-1beta production and the NF-kappaB signaling pathways. Mol. Cell. Biochem. 451, 145–153.
Kreutz, D., Sinthuvanich, C., Bileck, A., Janker, L., Muqaku, B., Slany, A., Gerner, C., 2018. Curcumin exerts its antitumor effects in a context dependent fashion. J. Proteomics 182, 65–72.
Lehrer, S., Rheinstein, P.H., 2015. Is Alzheimer's disease autoimmune inflammation of the brain that can be treated with nasal nonsteroidal anti-inflammatory drugs? Am. J. Alzheimers Dis. Other Demen. 30, 225–227.
Li, C., Chen, T., Zhou, H., Zhang, C., Feng, Y., Tang, F., Hoi, M.P., He, C., Zheng, Y., Lee, S.M., 2018. Schisantherin a attenuates neuroinflammation in activated microglia: role of Nrf2 activation through ERK phosphorylation. Cell. Physiol. Biochem. 47, 1769–1784.
Li, W., Suwanwela, N.C., Patumraj, S., 2017. Curcumin prevents reperfusion injury following ischemic stroke in rats via inhibition of NFkappaB, ICAM-1, MMP-9 and caspase-3 expression. Mol. Med. Rep. 16, 4710–4720.
Nair, S., Sobotka, K.S., Joshi, P., Gressens, P., Fleiss, B., Thornton, C., Mallard, C., Hagberg, H., 2019. Lipopolysaccharide-induced alteration of mitochondrial morphology induces a metabolic shift in microglia modulating the inflammatory response in vitro and in vivo. Glia 67, 1047–1061.
Patel, S.S., Udayabanu, M., 2017. Effect of natural products on diabetes associated neurological disorders. Rev. Neurosci. 28, 271–293.
Ransohoff, R.M., 2016. A polarizing question: do M1 and M2 microglia exist? Nat. Neurosci. 19, 987–991.
Ravelli, K.G., Santos, G.D., Dos Santos, N.B., Munhoz, C.D., Azzi-Nogueira, D., Campos, A.C., Pagano, R.L., Britto, L.R., Hernandes, M.S., 2019. Nox2-dependent neuroinflammation in an EAE model of multiple sclerosis. Transl. Neurosci. 10, 1–9.
Ren, M., Guo, Y., Wei, X., Yan, S., Qin, Y., Zhang, X., Jiang, F., Lou, H., 2018. TREM2 overexpression attenuates neuroinflammation and protects dopaminergic neurons in experimental models of Parkinson's disease. Exp. Neurol. 302, 205–213.
Rosciszewski, G., Cadena, V., Murta, V., Lukin, J., Villarreal, A., Roger, T., Ramos, A.J., 2018. Toll-like receptor 4 (TLR4) and triggering receptor expressed on myeloid Cells-2 (TREM-2) activation balance astrocyte polarization into a proinflammatory phenotype. Mol. Neurobiol. 55, 3875–3888.
Sharman, M.J., Verdile, G., Kirubakaran, S., Parenti, C., Singh, A., Watt, G., Karl, T., Chang, D., Li, C.G., Munch, G., 2019. Targeting inflammatory pathways in Alzheimer's disease: a focus on natural products and Phytomedicines. CNS Drugs 33, 457–480.
Shi, H., Wang, X.L., Quan, H.F., Yan, L., Pei, X.Y., Wang, R., Peng, X.D., 2019. Effects of betaine on LPS-Stimulated activation of microglial M1/M2 phenotypes by suppressing TLR4/NF-kappaB pathways in N9 cells. Molecules 24.
Subhramanyam, C.S., Wang, C., Hu, Q., Dheen, S.T., 2019. Microglia-mediated neuroinflammation in neurodegenerative diseases. Semin. Cell Dev. Biol.
Takahashi, K., Rochford, C.D., Neumann, H., 2005. Clearance of apoptotic neurons without inflammation by microglial triggering receptor expressed on myeloid cells-2. J. Exp. Med. 201, 647–657.
Tang, M., Taghibiglou, C., 2017. The mechanisms of action of curcumin in alzheimer's disease. J. Alzheimers Dis. 58, 1003–1016.
Tang, Y., Le, W., 2016. Differential roles of M1 and M2 microglia in neurodegenerative diseases. Mol. Neurobiol. 53, 1181–1194.
Tizabi, Y., Hurley, L.L., Qualls, Z., Akinfiresoye, L., 2014. Relevance of the anti-inflammatory properties of curcumin in neurodegenerative diseases and depression. Molecules 19, 20864–20879.
Wan, J., Shan, Y., Fan, Y., Fan, C., Chen, S., Sun, J., Zhu, L., Qin, L., Yu, M., Lin, Z., 2016. NF-kappaB inhibition attenuates LPS-induced TLR4 activation in monocyte cells. Mol. Med. Rep. 14, 4505–4510.
Wu, F., Luo, T., Mei, Y., Liu, H., Dong, J., Fang, Y., Peng, J., Guo, Y., 2018. Simvastatin alters M1/M2 polarization of murine BV2 microglia via Notch signaling. J. Neuroimmunol. 316, 56–64.
Xiong, X., Xu, L., Wei, L., White, R.E., Ouyang, Y.B., Giffard, R.G., 2015. IL-4 is required for sex differences in vulnerability to focal ischemia in mice. Stroke 46, 2271–2276.
Yan, A., Liu, Z., Song, L., Wang, X., Zhang, Y., Wu, N., Lin, J., Liu, Y., Liu, Z., 2018. Idebenone alleviates neuroinflammation and modulates microglial polarization in LPS-Stimulated BV2 cells and MPTP-Induced parkinson's disease mice. Front. Cell. Neurosci. 12, 529.
Yang, J., Ding, S., Huang, W., Hu, J., Huang, S., Zhang, Y., Zhuge, Q., 2016. Interleukin-4 ameliorates the functional recovery of intracerebral hemorrhage through the alternative activation of Microglia/Macrophage. Front. Neurosci. 10, 61.
Yang, Q.Q., Zhou, J.W., 2019. Neuroinflammation in the central nervous system: symphony of glial cells. Glia 67, 1017–1035.
Zhang, B., Wei, Y.Z., Wang, G.Q., Li, D.D., Shi, J.S., Zhang, F., 2018a. Targeting MAPK pathways by naringenin modulates microglia M1/M2 polarization in Lipopolysaccharide-Stimulated cultures. Front. Cell. Neurosci. 12, 531.
Zhang, Y., Fang, M., Sun, Y., Zhang, T., Shi, N., Li, J., Jin, L., Liu, K., Fu, J., 2018b. Curcumin attenuates cerebral ischemia injury in Sprague-Dawley rats and PC12 cells by suppressing overactivated autophagy. J. Photochem. Photobiol. B, Biol. 184, 1–6.
Zhang, Y., He, M.L., 2017. Deferoxamine enhances alternative activation of microglia and inhibits amyloid beta deposits in APP/PS1 mice. Brain Res. 1677, 86–92.
Zhou, J., Yu, W., Zhang, M., Tian, X., Li, Y., Lu, Y., 2019. Imbalance of microglial TLR4/TREM2 in LPS-Treated APP/PS1 transgenic mice: a potential link between Alzheimer's disease and systemic inflammation. Neurochem. Res. 44, 1138–1151.